Thermal Axion Cosmology

19th June 2015, Santander

Eleonora Di Valentino
Institut d'Astrophysique de Paris

Axions

The most elegant and promising solution of the so-called *strong CP problem* in Quantum Chromodynamics (QCD) was provided by Peccei and Quinn, adding a new global $U(1)_{PQ}$ symmetry. This is spontaneously broken at an energy scale f_a, generating a new spinless particle, the axion.

The axion can be copiously produced in the universe's early stages, both via thermal and non-thermal processes.

- Thermal axions with sub-eV masses contribute to the hot dark matter component of the universe, as neutrinos.

E. Giusarma, E. Di Valentino, M. Lattanzi, A. Melchiorri and O. Mena, Phys. Rev. D90 (2014), 043507.

- Axion-like particles produced non-thermally, as for example by the misalignment mechanism, instead were postulated as natural candidates for the cold dark matter component.

E. Di Valentino, E. Giusarma, M. Lattanzi, A. Melchiorri and O. Mena, Phys. Rev. D90 (2014), 043534.

Thermal Axions

For axion thermalization purposes, only the axion-pion interaction will be relevant.

$$\pi + \pi \rightarrow \pi + a$$

The axion particles are very similar to neutral pions, but their masses and interactions strengths are suppressed by a factor of order f_π/f_a, respect to the pion case:

$$m_a = \frac{f_\pi m_\pi}{f_a} \frac{\sqrt{R}}{1+R} = 0.6 \text{ eV } \frac{10^7 \text{ GeV}}{f_a}$$

where R=0.553±0.043 is the up-to-down quark masses ratio and f_π=93MeV is the pion decay constant.

Thermal Axions

Massive thermal axions will affect the cosmological observables in a very similar way to that induced by the presence of neutrino masses.

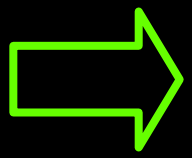

When axions are relativistic, will contribute to the dark radiation content of the universe, increasing the effective number of relativistic degrees of freedom N_{eff}.

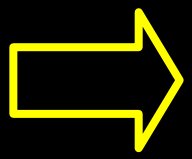

When they become non-relativistic, will only cluster at scales larger than their free streaming scale, suppressing therefore structure formation at small scales, and affecting the large scale structures.
Axion mass will also lead to a signature in the CMB photon temperature anisotropies via the early integrated Sachs-Wolfe effect.

Thermal axions, when are relativistic, will contribute to the hot dark matter component of the universe, so to the extra radiation component, by an amount given by:

$$\Delta N_{\rm eff} = \frac{4}{7}\left(\frac{3}{2}\frac{n_a}{n_\nu}\right)^{4/3}$$

We computed the current axion number density n_a, related to the present photon density by:

$$n_a = \frac{g_{\star S}(T_0)}{g_{\star S}(T_D)} \times \frac{n_\gamma}{2}$$

and the axion decoupling temperature T_D, that will be a function of the axion mass m_a, numerically solving the freeze out equation of the axion-pion interaction:

$$\Gamma(T_D) = H(T_D)$$

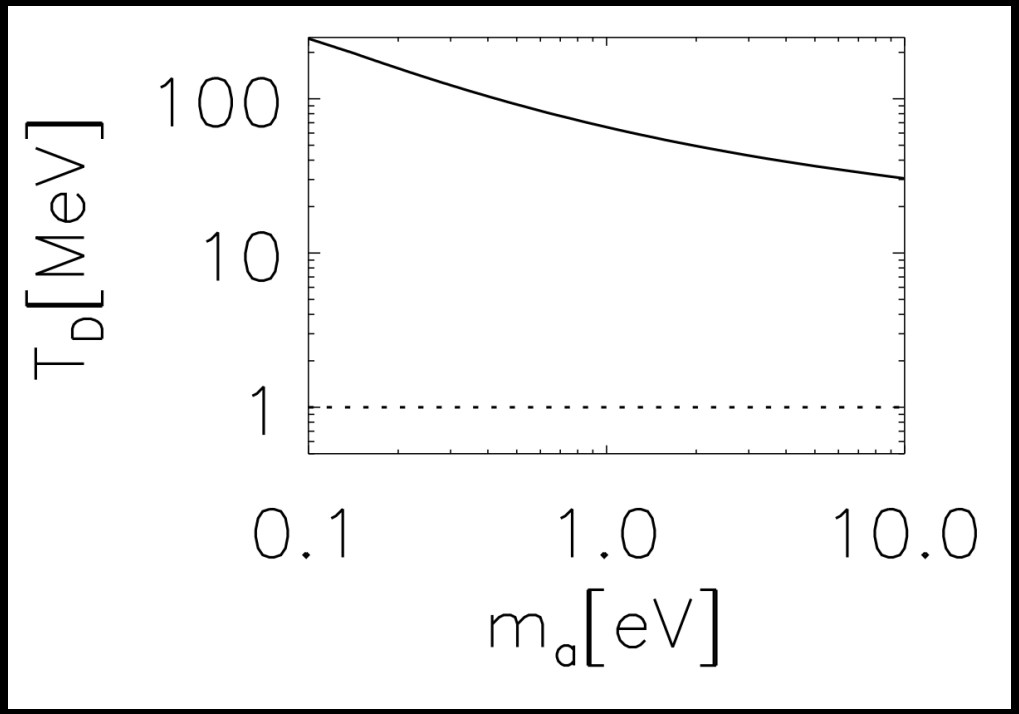

The temperature of decoupling is a function of the axion mass (solid curve). The higher the axion mass, the lower the temperature of decoupling is.

The axion contribution to the extra dark radiation content of the universe, as a function of the axion mass. Notice that the extra dark radiation arising from a 1 eV axion is still compatible (at 95% CL) with the most recent measurements of Neff from the Planck 2015 data release.

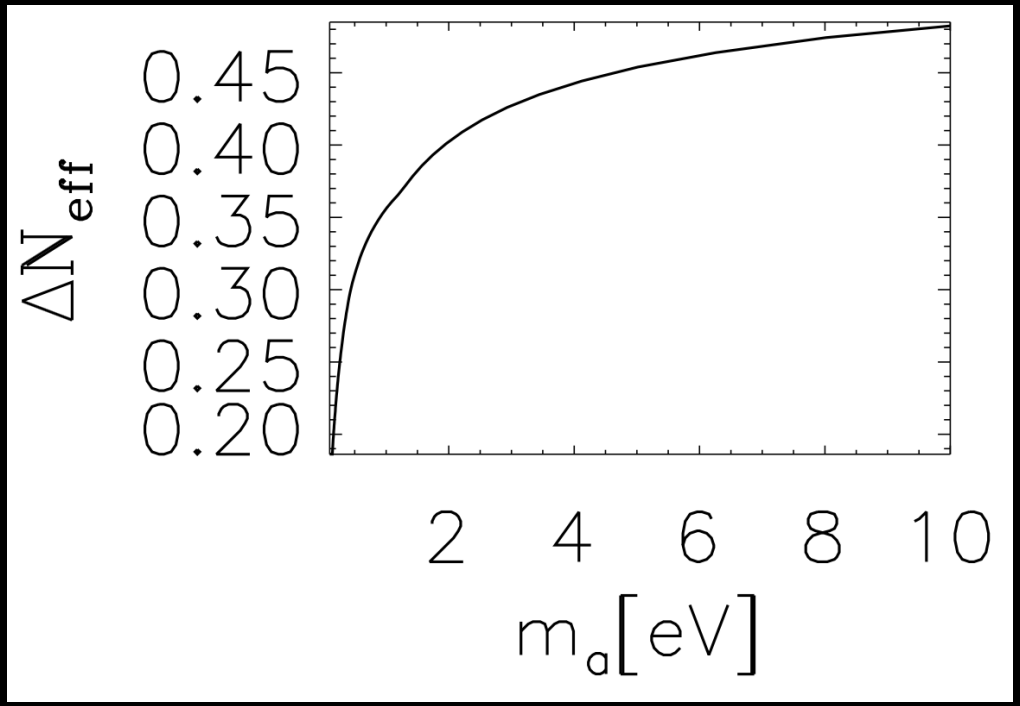

E. Di Valentino, S. Gariazzo, E. Giusarma and O. Mena, Phys. Rev. D. 91, 123505 (2015), arXiv:1503.00911

When massive axion particles become non-relativistic, will contribute to the matter density of the universe:

$$\Omega_a h^2 = \frac{m_a n_a}{1.054 \cdot 10^4 \text{ eV cm}^{-3}} = \frac{m_a}{131 \text{ eV}} \left(\frac{10}{g_{\star S}(T_D)} \right)$$

However their effect is degenerate with massive neutrinos, in particular they are negatively correlated. In fact, an increase in the axion mass will increase the hot dark matter component, and in order to keep the total amount consistent with the data, the contribution to the hot dark matter from the neutrinos should be reduced.

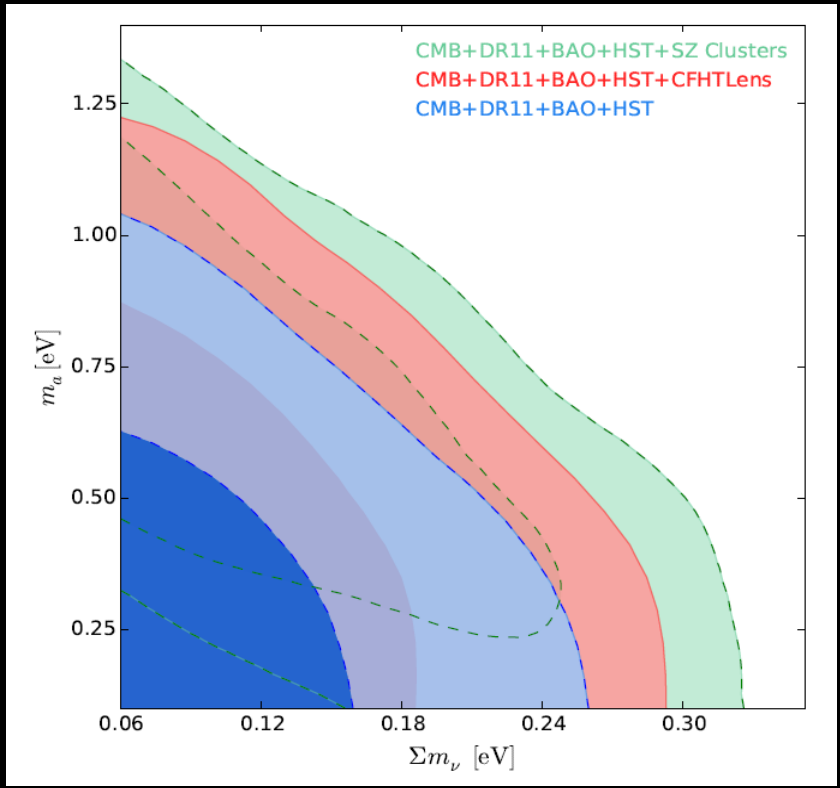

E. Giusarma, E. Di Valentino, M. Lattanzi, A. Melchiorri and O. Mena, Phys. Rev. D90 (2014), 043507

	CMB+DR11	CMB+DR11 +HST	CMB+DR11 +WZ	CMB+DR11 +WZ+HST	CMB+DR11 +WZ+BAO+HST	CMB+DR11 +BAO	CMB+DR11 +BAO+HST	CMB+DR11 +BAO+SNLS
Σm_ν [eV]	< 0.24	< 0.21	< 0.24	< 0.22	< 0.21	< 0.23	< 0.20	< 0.22
m_a [eV]	< 0.79	< 0.77	< 0.65	< 0.62	< 0.59	< 0.74	< 0.75	< 0.76
SZ Clusters & CFHTLensing								
Σm_ν [eV]	< 0.36	< 0.27	$0.21^{+013}_{-0.13}$	< 0.32	< 0.30	< 0.31	< 0.28	< 0.31
m_a [eV]	< 1.08	< 1.09	< 0.88	< 0.81	< 0.77	< 1.12	$0.63^{+0.47}_{-0.49}$	$0.58^{+0.50}_{-0.48}$
SZ Clusters								
Σm_ν [eV]	< 0.36	< 0.27	$0.20^{+013}_{-0.14}$	< 0.32	< 0.30	< 0.31	< 0.27	< 0.31
m_a [eV]	< 1.07	< 1.07	< 0.87	< 0.81	< 0.77	< 1.10	$0.62^{+0.46}_{-0.48}$	$0.57^{+0.50}_{-0.47}$

For these datasets we had only upper limits for the axion mass and the neutrino masses at 95% c.l..

E. Giusarma, E. Di Valentino, M. Lattanzi, A. Melchiorri and O. Mena, Phys. Rev. D90 (2014), 043507

	CMB+DR11	CMB+DR11 +HST	CMB+DR11 +WZ	CMB+DR11 +WZ+HST	CMB+DR11 +WZ+BAO+HST	CMB+DR11 +BAO	CMB+DR11 +BAO+HST	CMB+DR11 +BAO+SNLS
Σm_ν [eV]	< 0.24	< 0.21	< 0.24	< 0.22	< 0.21	< 0.23	< 0.20	< 0.22
m_a [eV]	< 0.79	< 0.77	< 0.65	< 0.62	< 0.59	< 0.74	< 0.75	< 0.76
SZ Clusters & CFHTLensing								
Σm_ν [eV]	< 0.36	< 0.27	$0.21^{+013}_{-0.13}$	< 0.32	< 0.30	< 0.31	< 0.28	< 0.31
m_a [eV]	< 1.08	< 1.09	< 0.88	< 0.81	< 0.77	< 1.12	$0.63^{+0.47}_{-0.49}$	$0.58^{+0.50}_{-0.48}$
SZ Clusters								
Σm_ν [eV]	< 0.36	< 0.27	$0.20^{+013}_{-0.14}$	< 0.32	< 0.30	< 0.31	< 0.27	< 0.31
m_a [eV]	< 1.07	< 1.07	< 0.87	< 0.81	< 0.77	< 1.10	$0.62^{+0.46}_{-0.48}$	$0.57^{+0.50}_{-0.47}$

For these datasets there was an evidence at more than 2σ for an axion mass of 0.6eV

E. Giusarma, E. Di Valentino, M. Lattanzi, A. Melchiorri and O. Mena, Phys. Rev. D90 (2014), 043507

	CMB+DR11	CMB+DR11 +HST	CMB+DR11 +WZ	CMB+DR11 +WZ+HST	CMB+DR11 +WZ+BAO+HST	CMB+DR11 +BAO	CMB+DR11 +BAO+HST	CMB+DR11 +BAO+SNLS
Σm_ν [eV]	< 0.24	< 0.21	< 0.24	< 0.22	< 0.21	< 0.23	< 0.20	< 0.22
m_a [eV]	< 0.79	< 0.77	< 0.65	< 0.62	< 0.59	< 0.74	< 0.75	< 0.76
SZ Clusters & CFHTLensing								
Σm_ν [eV]	< 0.36	< 0.27	$0.21^{+013}_{-0.13}$	< 0.32	< 0.30	< 0.31	< 0.28	< 0.31
m_a [eV]	< 1.08	< 1.09	< 0.88	< 0.81	< 0.77	< 1.12	$0.63^{+0.47}_{-0.49}$	$0.58^{+0.50}_{-0.48}$
SZ Clusters								
Σm_ν [eV]	< 0.36	< 0.27	$0.20^{+013}_{-0.14}$	< 0.32	< 0.30	< 0.31	< 0.27	< 0.31
m_a [eV]	< 1.07	< 1.07	< 0.87	< 0.81	< 0.77	< 1.10	$0.62^{+0.46}_{-0.48}$	$0.57^{+0.50}_{-0.47}$

The value of σ8 reported by cluster measurements and the value estimated from Planck CMB measurements show a tension at the ~ 2σ level. These discrepancies may arise due to the lack of a full understanding of the cluster mass calibrations. However, in extended cosmological models with non-zero neutrino masses these discrepancies are alleviated.

For these datasets there was an evidence at more than 3σ for a neutrino mass of 0.2eV

E. Giusarma, E. Di Valentino, M. Lattanzi, A. Melchiorri and O. Mena, Phys. Rev. D90 (2014), 043507

All the cosmological axion mass bounds to date have assumed the usual simple power law description for the primordial perturbations.
We want to constrain the mass of the thermal axion using a non-parametric description of the Primordial Power Spectrum of the scalar perturbations, in order to test the robustness of these bounds.
In fact, while the simplest models of inflation assume that the PPS has a scale-free power-law form, in general it could be more complicated, presenting various features or a scale dependence.
The energy scales at which the PPS was produced during inflation can not be directly tested. We can only infer the PPS by measuring the current matter power spectrum in the galaxy distribution and the power spectrum of the CMB fluctuations, that is the convolution of the PPS with the transfer function. The assumption of an underlying cosmological model is a mandatory first step in order to compute the transfer function.

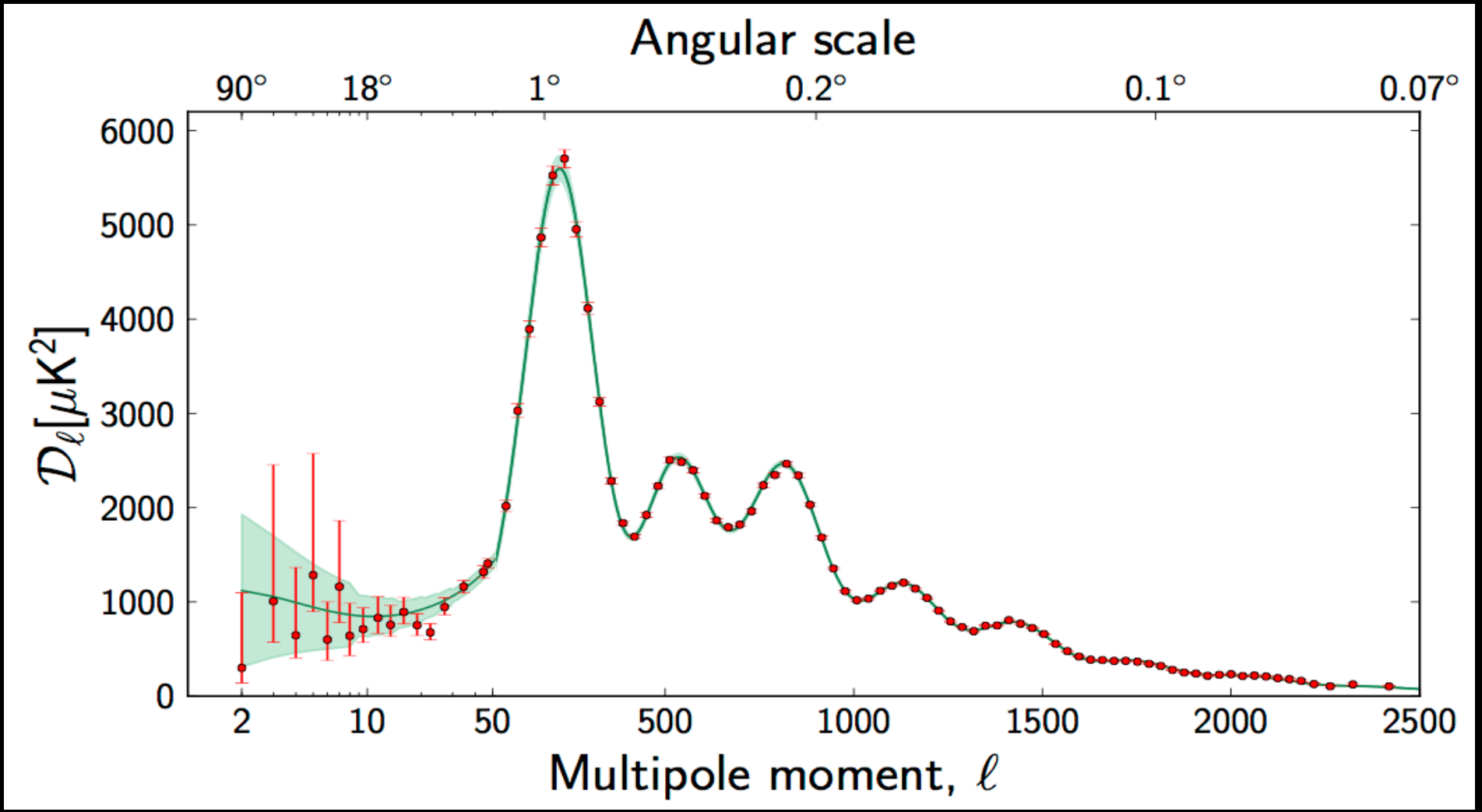

Planck collaboration, 2013

The standard cosmological model seems to fail at very low-l.
In fact, the low-l spectrum of the temperature perturbations measured by the Planck experiment shows a dip in the power around l=22, that cannot be explained in the standard cosmological scenario.

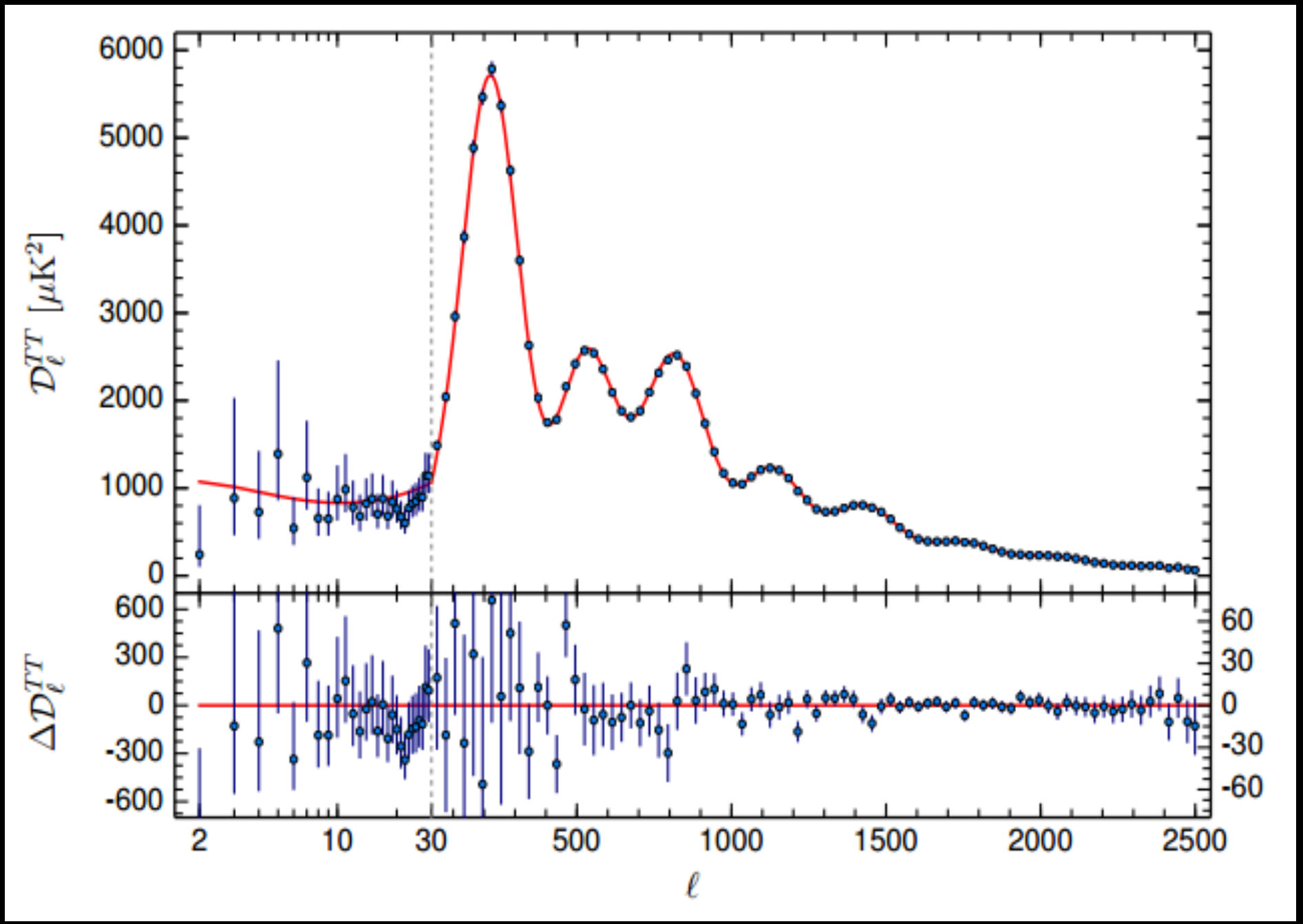

Planck collaboration, 2015

We consider a thermal axion scenario, allowing the PPS to assume a more general shape than the usual power law description. This may allow us to remove possible biases in the thermal axion mass induced by the PPS power-law assumptions.

$$\Delta^2_{\mathcal{R}}(k) = \Delta^2_{\mathcal{R}}(k_0) \left(\frac{k}{k_0}\right)^{n_s - 1 + (\alpha_s/2)\ln(k/k_0)}$$

Among the large number of possibilities, we decided to use the "piecewise cubic Hermite interpolating polynomial" (PCHIP). This modified spline function interpolates the PPS values in a series of nodes at fixed position, and is defined to preserve the original monotonicity of the point series that is interpolated.

$$P_s(k) = P_0 \times \texttt{PCHIP}(k; P_{s,1}, \ldots, P_{s,12})$$

where $P_0 = 2.36 \times 10^{-9}$ and $P_{s,j}$ is the value of the PPS at the node k_j divided by P_0.

We adopt the PCHIP interpolating function
in order to avoid spurious oscillations
of the interpolating function between the nodes which is
often obtained in spline interpolations.

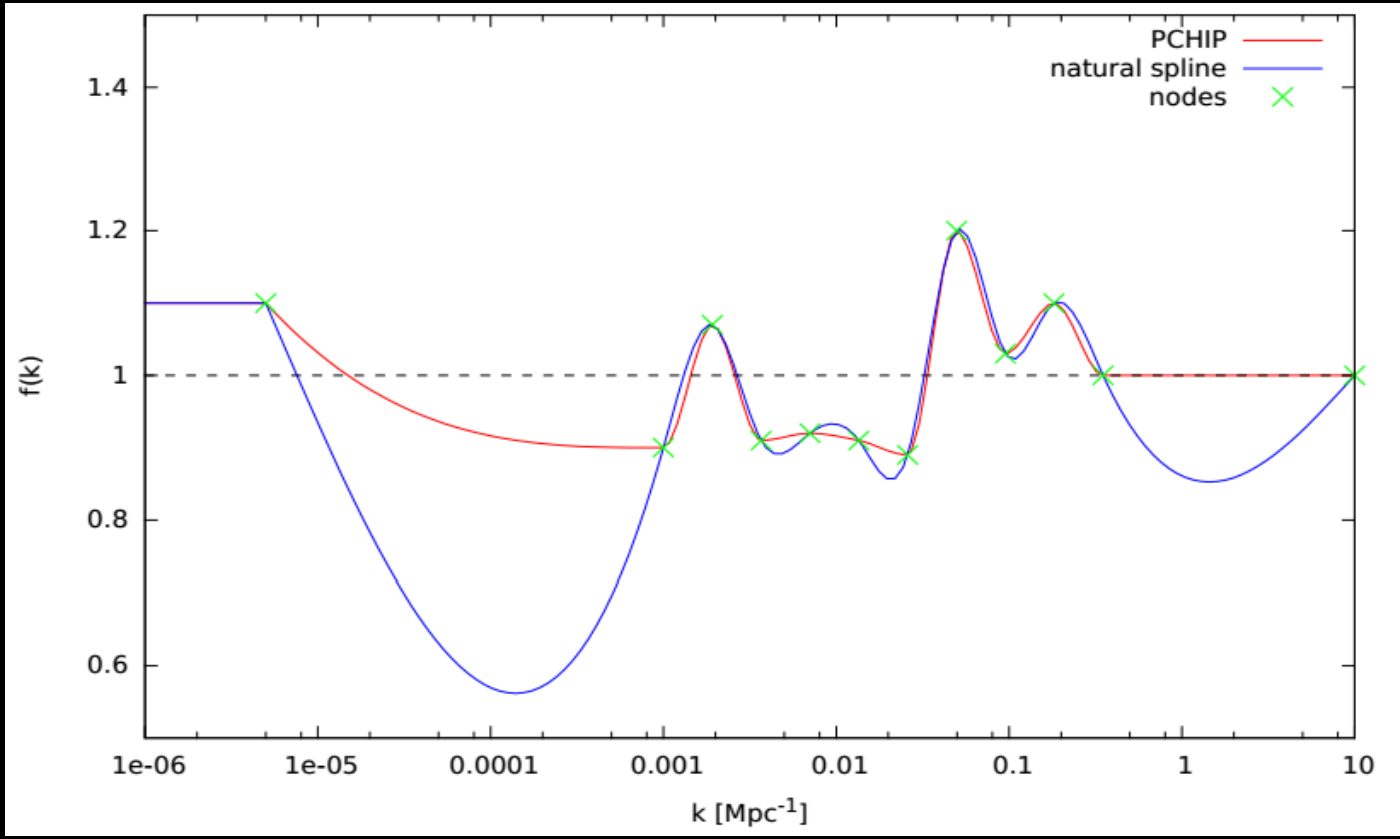

S. Gariazzo et al., arXiv:1412.7405v1

This problem occurs because a natural cubic spline requires the values of the function, the first and the second derivatives to be continuous in the nodes. In this way there is not a local control, and the interpolating curve is affected by the change of a single point.

Local control of the interpolating curve can be achieved by relaxing the requirement of continuity of the second derivatives in the nodes and using the resulting freedom to adjust the first derivatives with a local prescription, as in the PCHIP parameterization.

The PCHIP function is constructed in order to preserve the shape of the set of points to be interpolated preserving the local monotonicity.

To describe the scalar PPS with the PCHIP function, we only need to give the values of the PPS in a discrete number of nodes and to interpolate among them. Following S. Gariazzo et al., arXiv:1412.7405v1, we use 12 nodes which span a wide range of k values:

$$
\begin{aligned}
k_1 &= 5 \times 10^{-6}\,\mathrm{Mpc}^{-1}, \\
k_2 &= 10^{-3}\,\mathrm{Mpc}^{-1}, \\
k_j &= k_2 (k_{11}/k_2)^{(j-2)/9} \quad \text{for} \quad j \in [3, 10], \\
k_{11} &= 0.35\,\mathrm{Mpc}^{-1}, \\
k_{12} &= 10\,\mathrm{Mpc}^{-1}.
\end{aligned}
$$

The range (k_2, k_{11}) is well constrained from the data and we choose equally spaced nodes in the logarithmic scale. The nodes k_1 and k_{12} are used to parameterize a non-constant behavior of the PPS outside this well constrained range.

The behavior of PPS, is well constrained by the cosmological analysis between the range k2=0.001 Mpc^{-1} and k11=0.3 Mpc^{-1}.
In k1 and k12, the PPS has only upper limits, due to the absence of measurements at these wavenumbers.

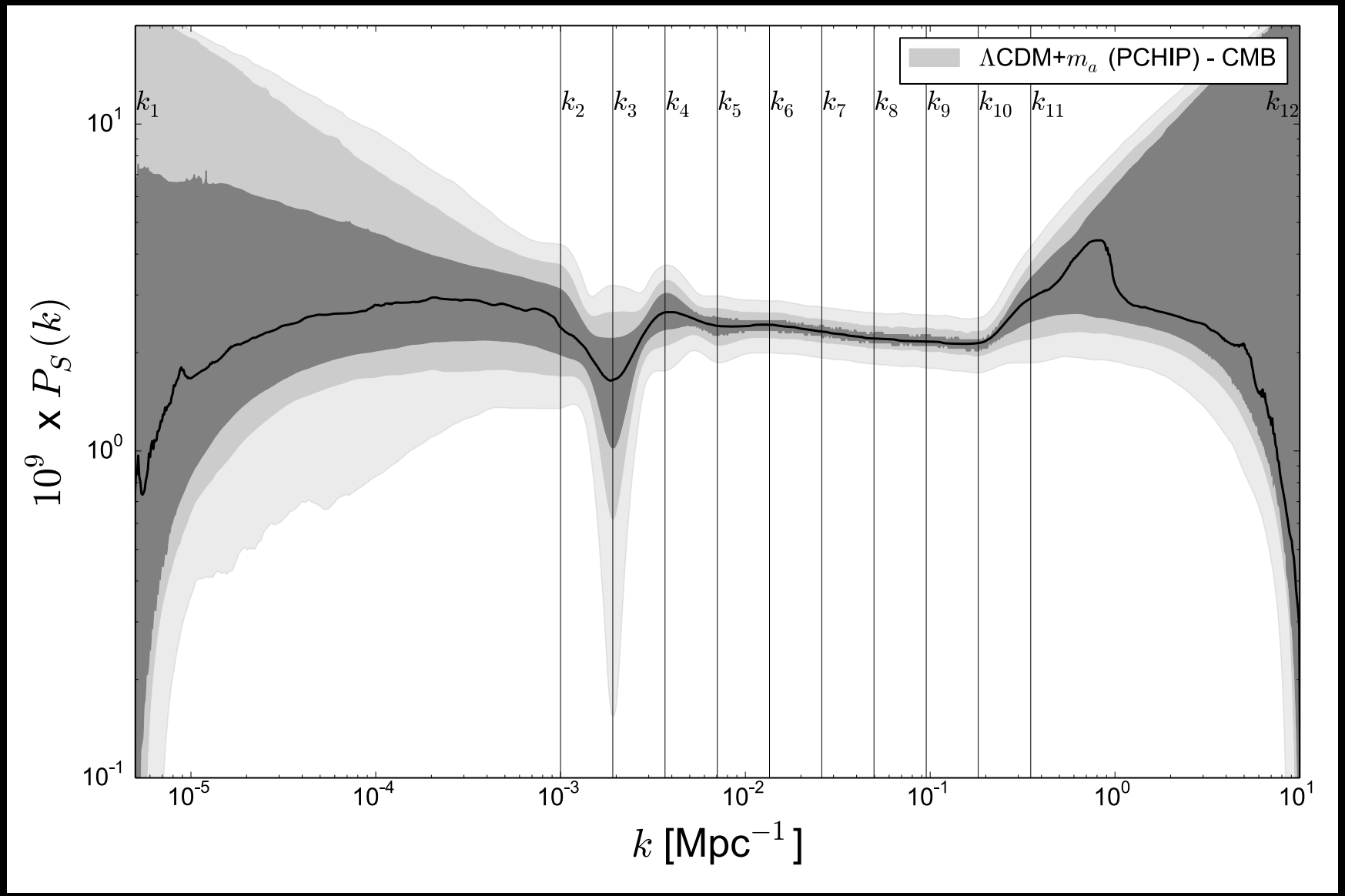

E. Di Valentino, S. Gariazzo, E. Giusarma and O. Mena, Phys. Rev. D. 91, 123505 (2015), arXiv:1503.00911

The PPS can be well approximated with a power-law parameterization between the range k_5=0.007 Mpc^{-1} and k_{10}=0.2 Mpc^{-1}. The values of the PPS in these nodes have only a few-percent uncertainty.

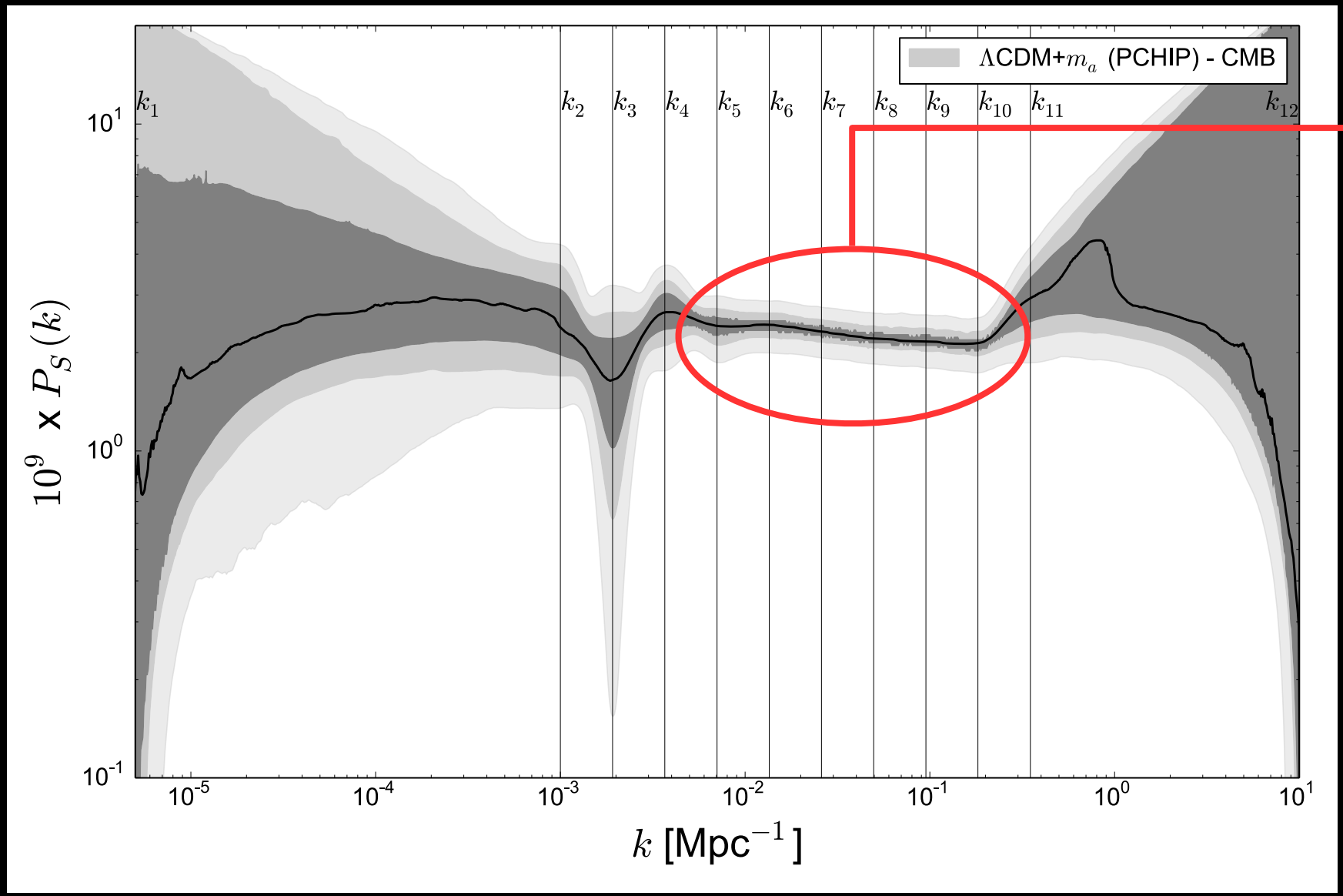

E. Di Valentino, S. Gariazzo, E. Giusarma and O. Mena, Phys. Rev. D. 91, 123505 (2015), arXiv:1503.00911

The PPS presents a clear dip a k_3=0.002 Mpc^{-1}, with a statistical significance at more than 2σ, and a small bump a k_4=0.0035 Mpc^{-1}, with a statistical significance of about 1σ. These major features are related to the dip in the temperature power spectrum around l=22 and to the slight excess around l=40.

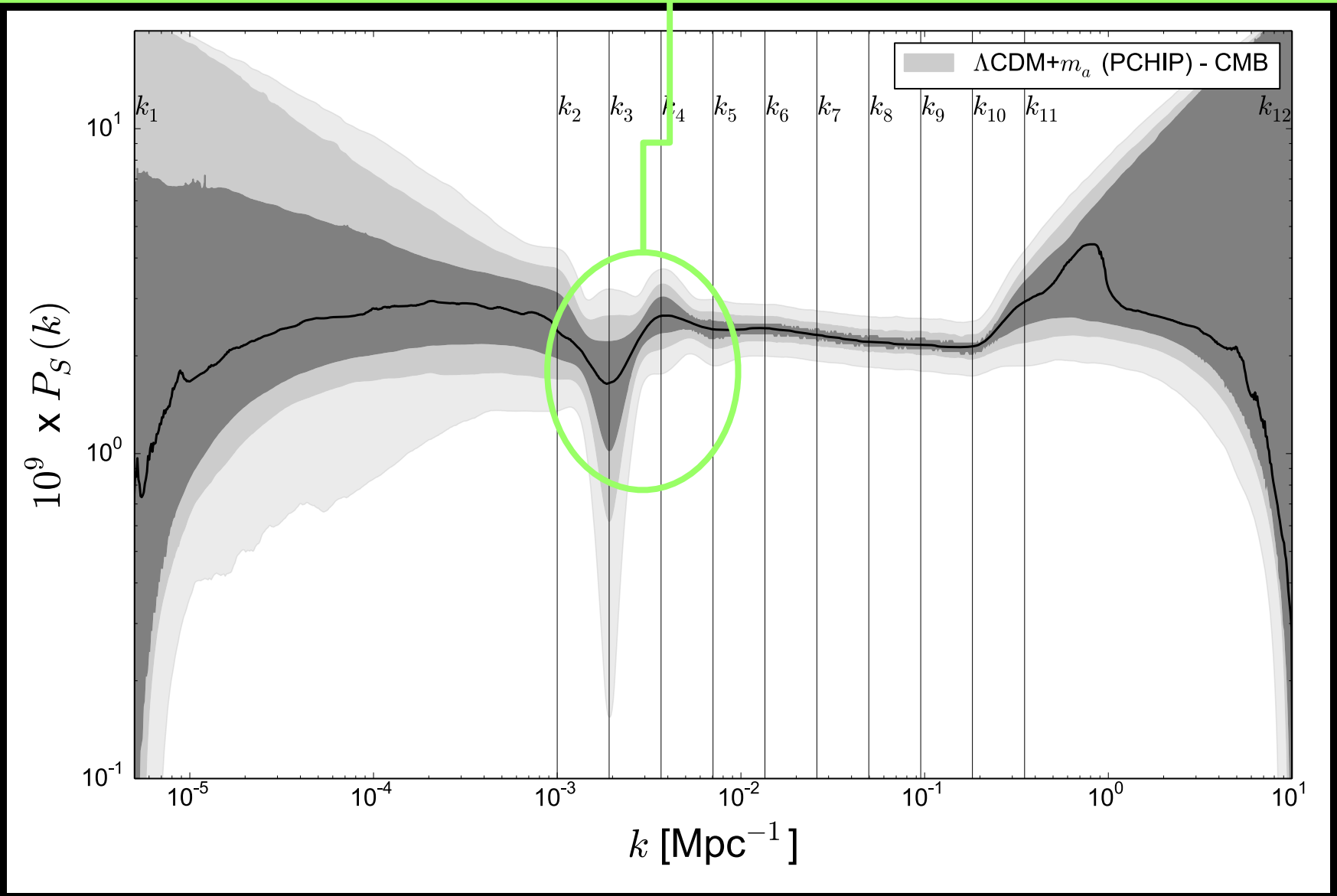

E. Di Valentino, S. Gariazzo, E. Giusarma and O. Mena, Phys. Rev. D. 91, 123505 (2015), arXiv:1503.00911

There are small hints for deviation of the PPS from the power-law form, even using different methods and datasets.

The behavior we found is in agreement with the natural cubic spline in R. de Putter et al. arXiv:1401.7022v2.

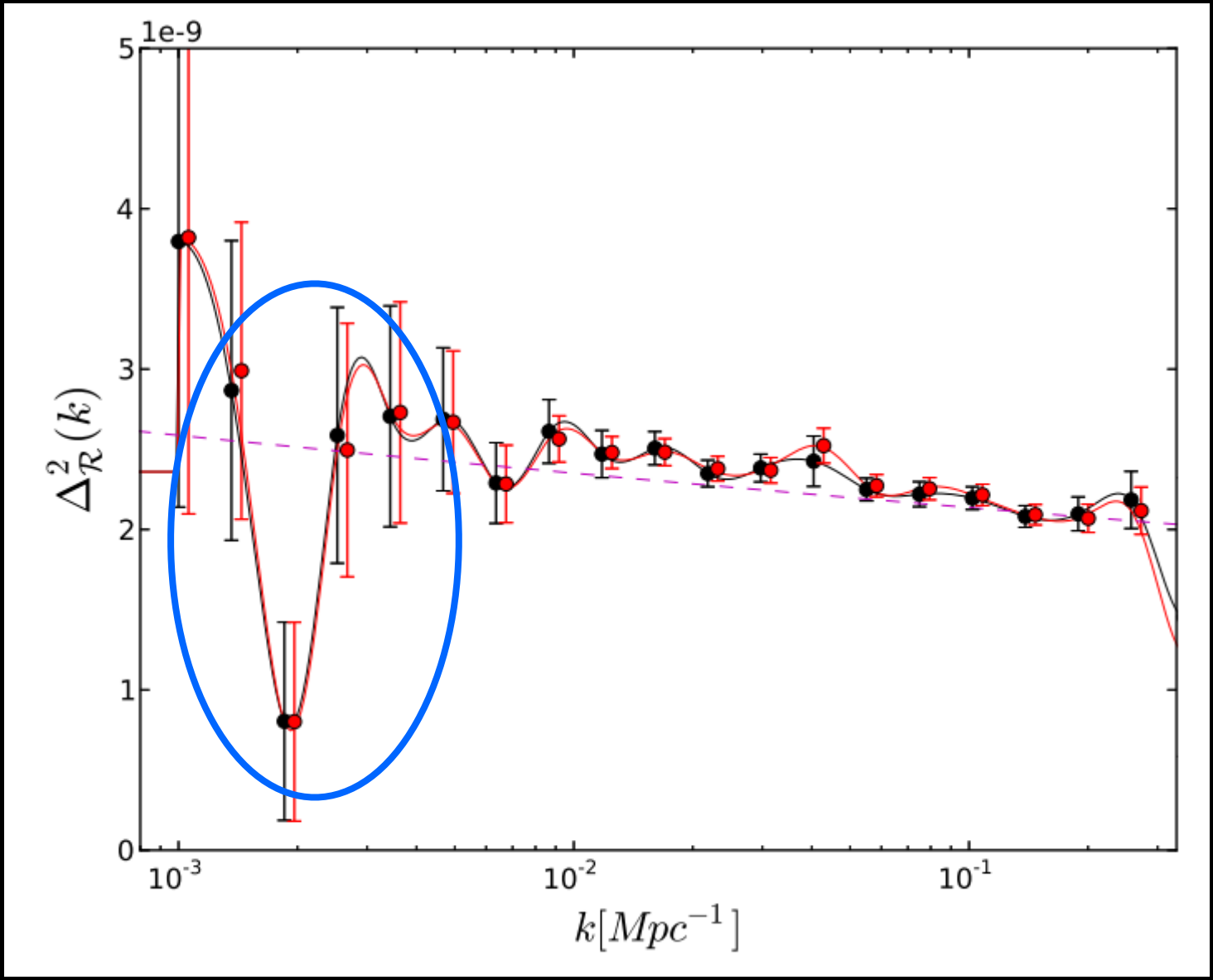

Finally, we obtain an increase of power at k ≃ 0.2 Mpc^{-1}, necessary to compensate the effects of the thermal axion mass in both the temperature anisotropies and the large scale structure of the universe.

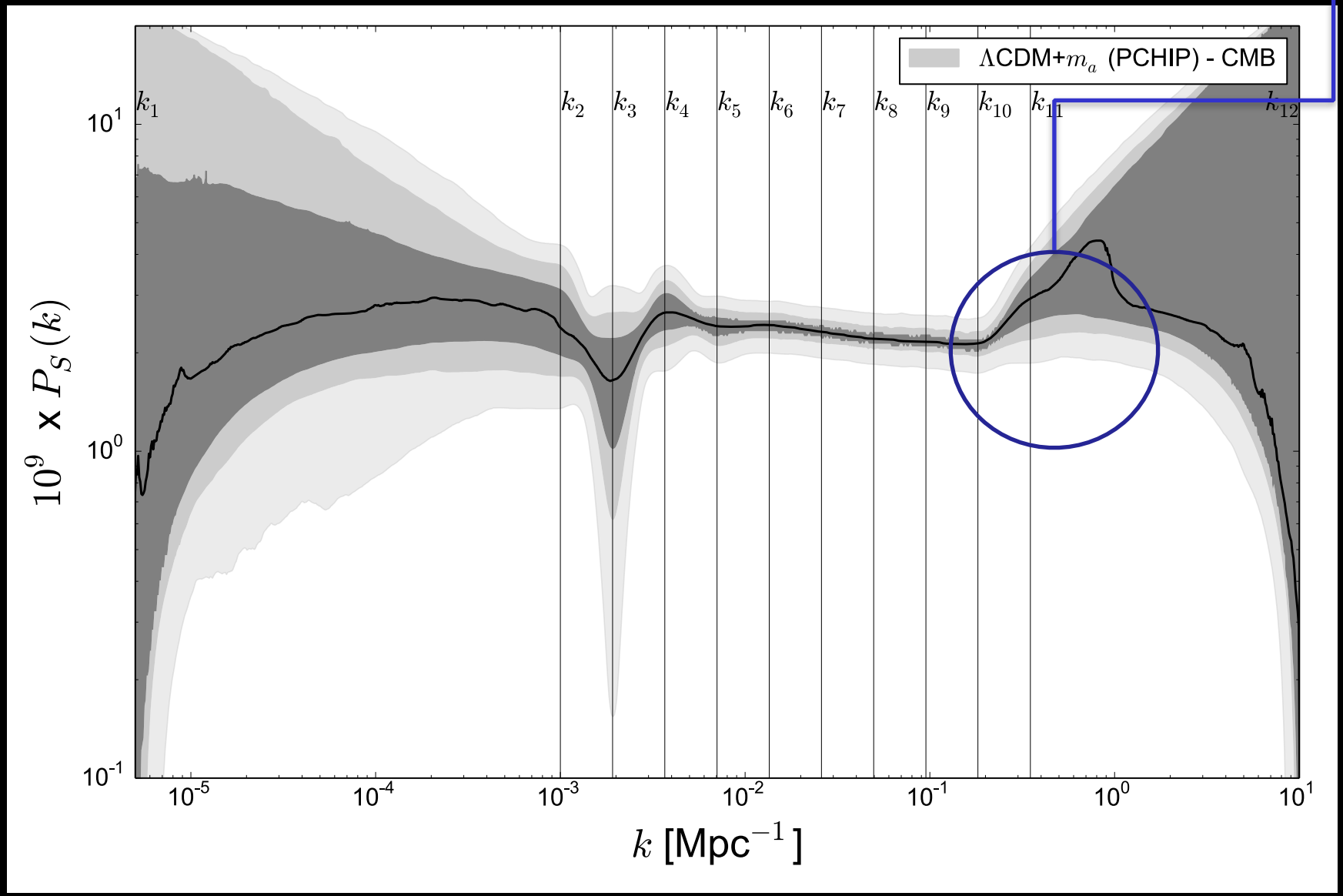

E. Di Valentino, S. Gariazzo, E. Giusarma and O. Mena, Phys. Rev. D. 91, 123505 (2015), arXiv:1503.00911

95% c.l.

	CMB	CMB+HST	CMB+BAO	CMB+BAO +HST	CMB+BAO HST+CFHT	CMB+BAO +HST+PSZ (fixed bias)	CMB+BAO +HST+PSZ
$\Omega_c h^2$	$0.127^{+0.007}_{-0.007}$	$0.122^{+0.006}_{-0.006}$	$0.122^{+0.003}_{-0.003}$	$0.121^{+0.003}_{-0.003}$	$0.120^{+0.003}_{-0.003}$	$0.118^{+0.002}_{-0.002}$	$0.119^{+0.003}_{-0.004}$
m_a [eV]	Unconstrained	< 1.31	< 0.89	< 0.91	< 1.29	$1.00^{+0.50}_{-0.48}$	$0.93^{+0.70}_{-0.71}$
σ_8	$0.788^{+0.079}_{-0.086}$	$0.821^{+0.052}_{-0.074}$	$0.827^{+0.044}_{-0.057}$	$0.825^{+0.045}_{-0.059}$	$0.793^{+0.049}_{-0.058}$	$0.760^{+0.023}_{-0.022}$	$0.767^{+0.046}_{-0.044}$
$\Omega_{\rm m}$	$0.369^{+0.070}_{-0.065}$	$0.314^{+0.045}_{-0.039}$	$0.308^{+0.016}_{-0.015}$	$0.304^{+0.016}_{-0.014}$	$0.302^{+0.016}_{-0.015}$	$0.304^{+0.016}_{-0.015}$	$0.304^{+0.016}_{-0.016}$
$P_{s,1}$	< 8.13	< 8.17	< 7.91	< 8.06	< 7.85	< 8.09	< 8.11
$P_{s,2}$	$1.09^{+0.42}_{-0.35}$	$1.01^{+0.43}_{-0.35}$	$1.01^{+0.40}_{-0.32}$	$0.99^{+0.42}_{-0.33}$	$1.02^{+0.43}_{-0.34}$	$1.01^{+0.42}_{-0.33}$	$1.05^{+0.43}_{-0.38}$
$P_{s,3}$	$0.68^{+0.39}_{-0.36}$	$0.71^{+0.39}_{-0.39}$	$0.71^{+0.39}_{-0.37}$	$0.72^{+0.39}_{-0.38}$	$0.69^{+0.39}_{-0.37}$	$0.70^{+0.40}_{-0.38}$	$0.69^{+0.40}_{-0.39}$
$P_{s,4}$	$1.14^{+0.24}_{-0.22}$	$1.15^{+0.24}_{-0.22}$	$1.15^{+0.23}_{-0.21}$	$1.15^{+0.23}_{-0.20}$	$1.15^{+0.23}_{-0.21}$	$1.15^{+0.23}_{-0.21}$	$1.15^{+0.22}_{-0.21}$
$P_{s,5}$	$1.02^{+0.11}_{-0.10}$	$1.01^{+0.11}_{-0.11}$	$1.00^{+0.11}_{-0.10}$	$1.00^{+0.11}_{-0.10}$	$0.99^{+0.11}_{-0.10}$	$0.99^{+0.11}_{-0.10}$	$0.99^{+0.11}_{-0.11}$
$P_{s,6}$	$1.03^{+0.08}_{-0.07}$	$1.00^{+0.08}_{-0.07}$	$1.00^{+0.08}_{-0.07}$	$1.00^{+0.08}_{-0.07}$	$0.98^{+0.07}_{-0.06}$	$0.98^{+0.07}_{-0.07}$	$0.98^{+0.08}_{-0.07}$
$P_{s,7}$	$0.99^{+0.07}_{-0.06}$	$0.98^{+0.08}_{-0.07}$	$0.98^{+0.07}_{-0.07}$	$0.98^{+0.08}_{-0.07}$	$0.96^{+0.07}_{-0.06}$	$0.95^{+0.07}_{-0.06}$	$0.96^{+0.07}_{-0.06}$
$P_{s,8}$	$0.94^{+0.06}_{-0.06}$	$0.95^{+0.08}_{-0.07}$	$0.95^{+0.07}_{-0.06}$	$0.95^{+0.08}_{-0.07}$	$0.94^{+0.07}_{-0.06}$	$0.94^{+0.07}_{-0.06}$	$0.94^{+0.07}_{-0.06}$
$P_{s,9}$	$0.92^{+0.06}_{-0.05}$	$0.94^{+0.08}_{-0.06}$	$0.94^{+0.07}_{-0.06}$	$0.94^{+0.08}_{-0.06}$	$0.93^{+0.07}_{-0.06}$	$0.93^{+0.07}_{-0.06}$	$0.94^{+0.07}_{-0.06}$
$P_{s,10}$	$0.90^{+0.06}_{-0.06}$	$0.91^{+0.08}_{-0.07}$	$0.91^{+0.07}_{-0.06}$	$0.91^{+0.08}_{-0.06}$	$0.90^{+0.07}_{-0.06}$	$0.90^{+0.07}_{-0.06}$	$0.90^{+0.07}_{-0.07}$
$P_{s,11}$	$1.25^{+0.30}_{-0.28}$	$1.24^{+0.32}_{-0.31}$	$1.23^{+0.31}_{-0.31}$	$1.24^{+0.31}_{-0.31}$	$1.22^{+0.30}_{-0.31}$	$1.22^{+0.32}_{-0.28}$	$1.23^{+0.31}_{-0.30}$
$P_{s,12}$	Unconstrained	Unconstrained	Unconstrained	Unconstrained	Unconstrained	Unconstrained	Unconstrained

E. Di Valentino, S. Gariazzo, E. Giusarma and O. Mena, Phys. Rev. D. 91, 123505 (2015), arXiv:1503.00911

95% c.l.	CMB	CMB+HST	CMB+BAO	CMB+BAO +HST	CMB+BAO HST+CFHT	CMB+BAO +HST+PSZ (fixed bias)	CMB+BAO +HST+PSZ
$\Omega_c h^2$	$0.127^{+0.007}_{-0.007}$	$0.122^{+0.006}_{-0.006}$	$0.122^{+0.003}_{-0.003}$	$0.121^{+0.003}_{-0.003}$	$0.120^{+0.003}_{-0.003}$	$0.118^{+0.002}_{-0.002}$	$0.119^{+0.003}_{-0.004}$
m_a [eV]	Unconstrained	< 1.31	< 0.89	< 0.91	< 1.29	$1.00^{+0.50}_{-0.48}$	$0.93^{+0.70}_{-0.71}$
σ_8	$0.788^{+0.079}_{-0.086}$	0.821	PCHIP PPS	$25^{+0.045}_{-0.059}$	$0.793^{+0.049}_{-0.058}$	$0.760^{+0.023}_{-0.022}$	$0.767^{+0.046}_{-0.044}$
Ω_m	$0.369^{+0.070}_{-0.065}$	$0.314^{}_{-0.039}$	$0.308^{}_{-0.015}$	$0.304^{+0.016}_{-0.014}$	$0.302^{+0.016}_{-0.015}$	$0.304^{+0.016}_{-0.015}$	$0.304^{+0.016}_{-0.016}$

	CMB	CMB+HST	CMB+BAO	CMB+BAO +HST	CMB+BAO HST+CFHT	CMB+BAO +HST+PSZ (fixed bias)	CMB+BAO +HST+PSZ
$\Omega_c h^2$	$0.124^{+0.006}_{-0.005}$	$0.124^{+0.005}_{-0.005}$	$0.122^{+0.004}_{-0.004}$	$0.121^{+0.004}_{-0.004}$	$0.120^{+0.003}_{-0.003}$	$0.119^{+0.003}_{-0.003}$	$0.120^{+0.003}_{-0.003}$
m_a [eV]	< 1.83	< 1.56	< 0.84	< 0.83	< 1.16	$0.80^{+0.53}_{-0.50}$	< 1.26
σ_8	$0.785^{+0.064}_{-0.083}$	Power Law PPS		041 048	$0.783^{+0.047}_{-0.054}$	$0.758^{+0.028}_{-0.029}$	$0.767^{+0.045}_{-0.045}$
Ω_m	$0.337^{+0.048}_{-0.044}$	$0.328^{+0.041}_{-0.039}$	$0.310^{+0.025}_{-0.023}$	$0.308^{+0.024}_{-0.023}$	$0.305^{+0.025}_{-0.024}$	$0.307^{+0.027}_{-0.026}$	$0.306^{+0.027}_{-0.025}$
$\log[10^{10} A_s]$	$3.10^{+0.05}_{-0.05}$	$3.10^{+0.05}_{-0.05}$	$3.10^{+0.05}_{-0.05}$	$3.10^{+0.05}_{-0.05}$	$3.10^{+0.05}_{-0.05}$	$3.09^{+0.05}_{-0.05}$	$3.09^{+0.05}_{-0.05}$
n_s	$0.961^{+0.014}_{-0.015}$	$0.963^{+0.013}_{-0.014}$	$0.968^{+0.011}_{-0.011}$	$0.969^{+0.011}_{-0.011}$	$0.971^{+0.011}_{-0.011}$	$0.973^{+0.011}_{-0.011}$	$0.972^{+0.011}_{-0.011}$

Except for the case in which CMB measurements are considered alone,
the thermal axion mass constraints do not change significantly.
This fact clearly states the robustness of the cosmological bounds on thermal axion masses.

E. Di Valentino, S. Gariazzo, E. Giusarma and O. Mena, Phys. Rev. D. 91, 123505 (2015), arXiv:1503.00911

95% c.l.

	CMB	CMB+HST	CMB+BAO	CMB+BAO +HST	CMB+BAO HST+CFHT	CMB+BAO +HST+PSZ (fixed bias)	CMB+BAO +HST+PSZ
$\Omega_c h^2$	$0.127^{+0.007}_{-0.007}$	$0.122^{+0.006}_{-0.006}$	$0.122^{+0.003}_{-0.003}$	$0.121^{+0.003}_{-0.003}$	$0.120^{+0.003}_{-0.003}$	$0.118^{+0.002}_{-0.002}$	$0.119^{+0.003}_{-0.004}$
m_a [eV]	Unconstrained	< 1.31	< 0.89	< 0.91	< 1.29	$1.00^{+0.50}_{-0.48}$	$0.93^{+0.70}_{-0.71}$
σ_8	$0.788^{+0.079}_{-0.086}$	$0.821^{+0.052}_{-0.074}$	$0.827^{+0.044}_{-0.057}$	$0.825^{+0.045}_{-0.059}$	$0.793^{+0.049}_{-0.058}$	$0.760^{+0.023}_{-0.022}$	$0.767^{+0.046}_{-0.044}$
Ω_m	$0.369^{+0.070}_{-0.065}$	$0.314^{+0.045}_{-0.039}$	$0.308^{+0.016}_{-0.015}$	0.304	PCHIP PPS	$0.304^{+0.016}_{-0.015}$	$0.304^{+0.016}_{-0.016}$

The addition to the CMB data of the HST prior on the Hubble constant provides a 95% CL upper limit on the thermal axion mass of 1.31 eV, while the further addition of the BAO measurements brings this constraint down to 0.91 eV, as these last data sets are directly sensitive to the free-streaming nature of the thermal axion. These upper bounds are very similar to the ones obtained when considering the standard power-law power spectrum.

	CMB	CMB+HST	CMB+BAO	CMB+BAO +HST	CMB+BAO HST+CFHT	CMB+BAO +HST+PSZ (fixed bias)	CMB+BAO +HST+PSZ
$\Omega_c h^2$	$0.124^{+0.006}_{-0.005}$	$0.124^{+0.005}_{-0.005}$	0.122^{+0}_{-0}	Power Law PPS		$0.119^{+0.003}_{-0.003}$	$0.120^{+0.003}_{-0.003}$
m_a [eV]	< 1.83	< 1.56	< 0.84	< 0.83	< 1.16	$0.80^{+0.53}_{-0.50}$	< 1.26
σ_8	$0.785^{+0.064}_{-0.083}$	$0.791^{+0.057}_{-0.076}$	$0.803^{+0.041}_{-0.048}$	$0.803^{+0.041}_{-0.048}$	$0.783^{+0.047}_{-0.054}$	$0.758^{+0.028}_{-0.029}$	$0.767^{+0.045}_{-0.045}$
Ω_m	$0.337^{+0.048}_{-0.044}$	$0.328^{+0.041}_{-0.039}$	$0.310^{+0.025}_{-0.023}$	$0.308^{+0.024}_{-0.023}$	$0.305^{+0.025}_{-0.024}$	$0.307^{+0.027}_{-0.026}$	$0.306^{+0.027}_{-0.025}$

E. Di Valentino, S. Gariazzo, E. Giusarma and O. Mena, Phys. Rev. D. 91, 123505 (2015), arXiv:1503.00911

95% c.l.	CMB	CMB+HST	CMB+BAO	CMB+BAO +HST	CMB+BAO HST+CFHT	CMB+BAO +HST+PSZ (fixed bias)	CMB+BAO +HST+PSZ
$\Omega_c h^2$	$0.127^{+0.007}_{-0.007}$	$0.122^{+0.006}_{-0.006}$	$0.122^{+0.003}_{-0.003}$	$0.121^{+0.003}_{-0.003}$	$0.120^{+0.003}_{-0.003}$	$0.118^{+0.002}_{-0.002}$	$0.119^{+0.003}_{-0.004}$
m_a [eV]	Unconstrained	< 1.31	< 0.89	< 0.91	< 1.29	$1.00^{+0.50}_{-0.48}$	$0.93^{+0.70}_{-0.71}$
σ_8	$0.788^{+0.079}_{-0.086}$	$0.821^{+0.052}_{-0.074}$	$0.827^{+0.044}_{-0.057}$	$0.825^{+0.045}_{-0.059}$	$0.793^{+0.049}_{-0.058}$	$0.760^{+0.023}_{-0.022}$	$0.767^{+0.046}_{-0.044}$
Ω_m	$0.369^{+0.070}_{-0.065}$	$0.314^{+0.045}_{-0.039}$	$0.308^{+0.016}_{-0.015}$	$0.304^{+0.016}_{-0.014}$	$0.302^{+0.016}_{-0.015}$	$0.304^{+0.016}_{-0.015}$	$0.304^{+0.016}_{-0.016}$

When adding the CFHT bounds on the $\sigma 8$-Ω_m relationship, the bounds on the thermal axion mass become weaker. The reason for that is due to the lower $\sigma 8$ values preferred by weak lensing measurements, that can be achieved by allowing for higher axion masses.

The larger the axion mass, the larger is the suppression of the matter power spectrum at small scales, leading consequently to a smaller value of the clustering parameter $\sigma 8$.

E. Di Valentino, S. Gariazzo, E. Giusarma and O. Mena, Phys. Rev. D. 91, 123505 (2015), arXiv:1503.00911

95% c.l.	CMB	CMB+HST	CMB+BAO	CMB+BAO +HST	CMB+BAO HST+CFHT	CMB+BAO +HST+PSZ (fixed bias)	CMB+BAO +HST+PSZ
$\Omega_c h^2$	$0.127^{+0.007}_{-0.007}$	$0.122^{+0.006}_{-0.006}$	$0.122^{+0.003}_{-0.003}$	$0.121^{+0.003}_{-0.003}$	$0.120^{+0.003}_{-0.003}$	$0.118^{+0.002}_{-0.002}$	$0.119^{+0.003}_{-0.004}$
m_a [eV]	Unconstrained	< 1.31	< 0.89	< 0.91	< 1.29	$1.00^{+0.50}_{-0.48}$	$0.93^{+0.70}_{-0.71}$
σ_8	$0.788^{+0.079}_{-0.086}$	$0.821^{+0.052}_{-0.074}$	$0.827^{+0.044}_{-0.057}$	$0.825^{+0.045}_{-0.059}$	$0.793^{+0.049}_{-0.058}$	$0.760^{+0.023}_{-0.022}$	$0.767^{+0.046}_{-0.044}$
Ω_m	$0.369^{+0.070}_{-0.065}$	$0.314^{+0.045}_{-0.039}$	$0.308^{+0.016}_{-0.015}$	$0.304^{+0.016}_{-0.014}$	PCHIP PPS	$^{+0.016}_{-0.015}$	$0.304^{+0.016}_{-0.016}$

Galaxy clusters represent an independent tool to probe the cosmological parameters. We used the cluster normalization condition as measured by the Planck Sunyaev-Zeldovich (PSZ) 2013 catalogue, $\sigma 8(\Omega m/0.27)^{0.3} = 0.78 \pm 0.01$, that fix the value of the bias parameter accordingly to the results arising from numerical simulations (fixed bias).

The addition of these (unrealistic) PSZ 2013 measurements on galaxy number counts favors an axion mass of ~ 1 eV (~ 0.80 eV) at ~ 4σ (~ 3σ) level.

	CMB	CMB+HST	CMB+BAO	CMB+BAO +HST	CMB+BAO HST+CFHT	CMB+BAO +HST+PSZ (fixed bias)	CMB+BAO +HST+PSZ
$\Omega_c h^2$	$0.124^{+0.006}_{-0.005}$	$0.124^{+0.005}_{-0.005}$	0.122^{+0}_{-0}	Power Law PPS		$0.119^{+0.003}_{-0.003}$	$0.120^{+0.003}_{-0.003}$
m_a [eV]	< 1.83	< 1.56	< 0.84	< 0.83	< 1.16	$0.80^{+0.53}_{-0.50}$	< 1.26
σ_8	$0.785^{+0.064}_{-0.083}$	$0.791^{+0.057}_{-0.076}$	$0.803^{+0.041}_{-0.048}$	$0.803^{+0.041}_{-0.048}$	$0.783^{+0.047}_{-0.054}$	$0.758^{+0.028}_{-0.029}$	$0.767^{+0.045}_{-0.045}$
Ω_m	$0.337^{+0.048}_{-0.044}$	$0.328^{+0.041}_{-0.039}$	$0.310^{+0.025}_{-0.023}$	$0.308^{+0.024}_{-0.023}$	$0.305^{+0.025}_{-0.024}$	$0.307^{+0.027}_{-0.026}$	$0.306^{+0.027}_{-0.025}$

E. Di Valentino, S. Gariazzo, E. Giusarma and O. Mena, Phys. Rev. D. 91, 123505 (2015), arXiv:1503.00911

95% c.l.	CMB	CMB+HST	CMB+BAO	CMB+BAO +HST	CMB+BAO HST+CFHT	CMB+BAO +HST+PSZ (fixed bias)	CMB+BAO +HST+PSZ
$\Omega_c h^2$	$0.127^{+0.007}_{-0.007}$	$0.122^{+0.006}_{-0.006}$	$0.122^{+0.003}_{-0.003}$	$0.121^{+0.003}_{-0.003}$	$0.120^{+0.003}_{-0.003}$	$0.118^{+0.002}_{-0.002}$	$0.119^{+0.003}_{-0.004}$
m_a [eV]	Unconstrained	< 1.31	< 0.89	< 0.91	< 1.29	$1.00^{+0.50}_{-0.48}$	$0.93^{+0.70}_{-0.71}$
σ_8	$0.788^{+0.079}_{-0.086}$	$0.821^{+0.052}_{-0.074}$	$0.827^{+0.044}_{-0.057}$	$0.825^{+0.045}_{-0.059}$	$0.793^{+0.049}_{-0.058}$	PCHIP PPS	$^{+0.046}_{-0.044}$
Ω_m	$0.369^{+0.070}_{-0.065}$	$0.314^{+0.045}_{-0.039}$	$0.308^{+0.016}_{-0.015}$	$0.304^{+0.016}_{-0.014}$	$0.302^{+0.016}_{-0.015}$		$^{+0.016}_{-0.016}$

However, as there exists a strong degeneracy between the value of the σ_8 parameter and the cluster mass bias, to use a more realistic approach for the cluster mass bias is crucial. So we decided to use also the PSZ 2013 measurements of the cluster normalization condition, without to fix the bias, $\sigma_8 (\Omega_m /0.27)^{0.3} = 0.764 \pm 0.025$, to see its impact.

The preference for a non-zero axion mass of 1 eV is only mild in the PCHIP PPS case, while in the case of a standard power-law PPS such an evidence completely disappears.

	CMB	CMB+HST	CMB+BAO	CMB+BAO +HST	CMB+BAO HST+CFHT	CMB+BAO +HST+PSZ (fixed bias)	CMB+BAO +HST+PSZ
$\Omega_c h^2$	$0.124^{+0.006}_{-0.005}$	$0.124^{+0.005}_{-0.005}$	$0.122^{+0.004}_{-0.004}$	$0.121^{+0.004}_{-0.004}$	0	Power Law PPS	$0.120^{+0.003}_{-0.003}$
m_a [eV]	< 1.83	< 1.56	< 0.84	< 0.83	< 1.16	$0.80^{+0.53}_{-0.50}$	< 1.26
σ_8	$0.785^{+0.064}_{-0.083}$	$0.791^{+0.057}_{-0.076}$	$0.803^{+0.041}_{-0.048}$	$0.803^{+0.041}_{-0.048}$	$0.783^{+0.047}_{-0.054}$	$0.758^{+0.028}_{-0.029}$	$0.767^{+0.045}_{-0.045}$
Ω_m	$0.337^{+0.048}_{-0.044}$	$0.328^{+0.041}_{-0.039}$	$0.310^{+0.025}_{-0.023}$	$0.308^{+0.024}_{-0.023}$	$0.305^{+0.025}_{-0.024}$	$0.307^{+0.027}_{-0.026}$	$0.306^{+0.027}_{-0.025}$

E. Di Valentino, S. Gariazzo, E. Giusarma and O. Mena, Phys. Rev. D. 91, 123505 (2015), arXiv:1503.00911

95% c.l.	CMB	CMB+HST	CMB+BAO	CMB+BAO +HST	CMB+BAO +HST+CFHT	CMB+BAO +HST+PSZ(fixed bias)	CMB+BAO +HST+PSZ
$\Omega_c h^2$	$0.130^{+0.008}_{-0.007}$	$0.125^{+0.006}_{-0.007}$	$0.121^{+0.003}_{-0.003}$	$0.121^{+0.003}_{-0.003}$	$0.119^{+0.003}_{-0.003}$	$0.118^{+0.003}_{-0.003}$	$0.118^{+0.003}_{-0.003}$
m_a [eV]	< 2.48	< 1.64	< 0.81	< 0.86	< 1.23	$0.81^{+0.59}_{-0.69}$	< 1.46
$\sum m_\nu$ [eV]	< 2.11	< 0.43	< 0.22	< 0.21	< 0.27	< 0.32	< 0.35
σ_8	$0.700^{+0.172}_{-0.202}$	$0.803^{+0.082}_{-0.091}$	$0.833^{+0.055}_{-0.058}$	$0.834^{+0.058}_{-0.064}$	$0.787^{+0.052}_{-0.055}$	$0.766^{+0.043}_{-0.044}$	$0.757^{+0.023}_{-0.022}$
Ω_m	$0.486^{+0.277}_{-0.193}$	$0.356^{+0.064}_{-0.062}$	$0.309^{+0.016}_{-0.015}$	$0.308^{+0.016}_{-0.015}$	$0.306^{+0.015}_{-0.015}$	$0.308^{+0.016}_{-0.016}$	$0.308^{+0.017}_{-0.016}$
$P_{s,1}$	< 8.01	< 8.13	< 7.00	< 8.17	< 7.59	< 8.29	< 8.18
$P_{s,2}$	$1.17^{+0.42}_{-0.38}$	$1.09^{+0.41}_{-0.37}$	$1.03^{+0.40}_{-0.35}$	$1.02^{+0.39}_{-0.34}$	$1.02^{+0.40}_{-0.32}$	$1.03^{+0.36}_{-0.34}$	$1.05^{+0.40}_{-0.36}$
$P_{s,3}$	$0.66^{+0.37}_{-0.35}$	$0.69^{+0.38}_{-0.37}$	$0.70^{+0.38}_{-0.38}$	$0.72^{+0.38}_{-0.37}$	$0.68^{+0.37}_{-0.33}$	$0.71^{+0.40}_{-0.39}$	$0.69^{+0.39}_{-0.37}$
$P_{s,4}$	$1.17^{+0.23}_{-0.23}$	$1.15^{+0.23}_{-0.22}$	$1.15^{+0.22}_{-0.21}$	$1.15^{+0.21}_{-0.21}$	$1.15^{+0.20}_{-0.19}$	$1.14^{+0.21}_{-0.20}$	$1.16^{+0.22}_{-0.21}$
$P_{s,5}$	$1.05^{+0.15}_{-0.14}$	$1.01^{+0.11}_{-0.10}$	$1.00^{+0.11}_{-0.10}$	$1.00^{+0.11}_{-0.10}$	$0.98^{+0.11}_{-0.10}$	$0.99^{+0.11}_{-0.10}$	$0.98^{+0.11}_{-0.10}$
$P_{s,6}$	$1.04^{+0.09}_{-0.08}$	$1.01^{+0.08}_{-0.07}$	$1.00^{+0.07}_{-0.07}$	$1.00^{+0.07}_{-0.07}$	$0.98^{+0.07}_{-0.06}$	$0.98^{+0.07}_{-0.07}$	$0.98^{+0.07}_{-0.07}$
$P_{s,7}$	$0.99^{+0.06}_{-0.06}$	$0.98^{+0.07}_{-0.06}$	$0.98^{+0.07}_{-0.07}$	$0.98^{+0.07}_{-0.07}$	$0.95^{+0.07}_{-0.06}$	$0.95^{+0.06}_{-0.06}$	$0.95^{+0.07}_{-0.06}$
$P_{s,8}$	$0.93^{+0.06}_{-0.05}$	$0.94^{+0.06}_{-0.06}$	$0.95^{+0.07}_{-0.07}$	$0.95^{+0.07}_{-0.07}$	$0.93^{+0.07}_{-0.05}$	$0.94^{+0.07}_{-0.06}$	$0.93^{+0.07}_{-0.06}$
$P_{s,9}$	$0.91^{+0.06}_{-0.05}$	$0.93^{+0.06}_{-0.06}$	$0.94^{+0.07}_{-0.06}$	$0.94^{+0.07}_{-0.06}$	$0.93^{+0.07}_{-0.06}$	$0.93^{+0.06}_{-0.06}$	$0.93^{+0.07}_{-0.06}$
$P_{s,10}$	$0.90^{+0.06}_{-0.06}$	$0.90^{+0.07}_{-0.06}$	$0.91^{+0.07}_{-0.07}$	$0.91^{+0.08}_{-0.07}$	$0.88^{+0.07}_{-0.06}$	$0.89^{+0.07}_{-0.07}$	$0.90^{+0.07}_{-0.07}$
$P_{s,11}$	$2.18^{+0.85}_{-0.77}$	$2.07^{+0.81}_{-0.80}$	$2.12^{+0.90}_{-0.86}$	$2.15^{+0.95}_{-0.94}$	$1.64^{+0.79}_{-0.75}$	$1.83^{+0.87}_{-0.86}$	$1.84^{+0.86}_{-0.87}$
$P_{s,12}$	Unconstrained	Unconstrained	Unconstrained	Unconstrained	Unconstrained	Unconstrained	Unconstrained

E. Di Valentino, S. Gariazzo, E. Giusarma and O. Mena, Phys. Rev. D. 91, 123505 (2015), arXiv:1503.00911

95% c.l.	CMB	CMB+HST	CMB+BAO	CMB+BAO +HST	CMB+BAO +HST+CFHT	CMB+BAO +HST+PSZ(fixed bias)	CMB+BAO +HST+PSZ
$\Omega_c h^2$	$0.130^{+0.008}_{-0.007}$	$0.125^{+0.006}_{-0.007}$	$0.121^{+0.003}_{-0.003}$	$0.121^{+0.003}_{-0.003}$	$0.119^{+0.003}_{-0.003}$	$0.118^{+0.003}_{-0.003}$	$0.118^{+0.003}_{-0.003}$
m_a [eV]	< 2.48	< 1.64	< 0.81	< 0.86	< 1.23	$0.81^{+0.59}_{-0.69}$	< 1.46
$\sum m_\nu$ [eV]	< 2.11	< 0.43	< 0.22	< 0.21	< 0.27	< 0.32	< 0.35
σ_8	$0.700^{+0.172}_{-0.202}$	$0.803^{+0.082}_{-0.091}$	$0.833^{+0.055}_{-0.058}$	$0.834^{+0.058}_{-0.064}$	$0.787^{+0.0}_{-0.0}$	PCHIP PPS	$0.757^{+0.023}_{-0.022}$
Ω_m	$0.486^{+0.277}_{-0.193}$	$0.356^{+0.064}_{-0.062}$	$0.309^{+0.016}_{-0.015}$	$0.308^{+0.016}_{-0.015}$	$0.306^{+0.015}_{-0.015}$	$0.308^{+0.016}_{-0.016}$	$0.308^{+0.017}_{-0.016}$

E. Di Valentino, S. Gariazzo, E. Giusarma and O. Mena, Phys. Rev. D. 91, 123505 (2015), arXiv:1503.00911

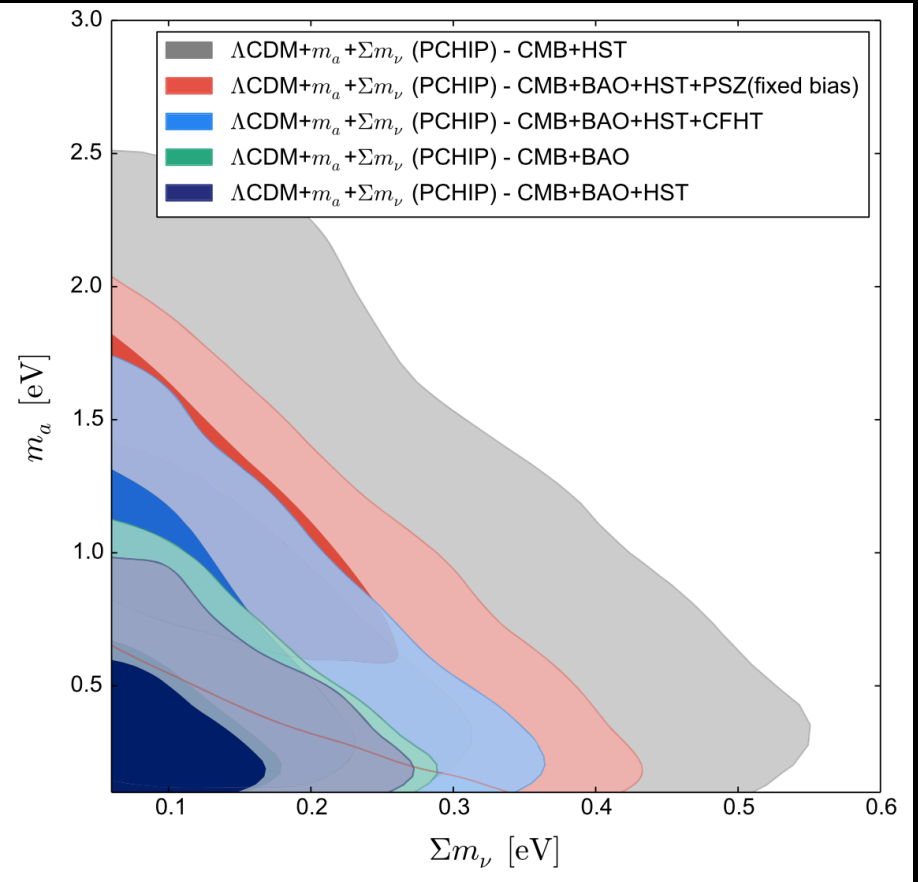

The preference for an axion mass of 1 eV disappears when adding the total neutrino mass, due to the strong correlation between the masses of the two hot thermal relics.

Conclusions:

- Axions provide the most elegant scenario to solve the strong CP problem, and may be produced in the early universe via both thermal and non-thermal processes.
- Thermal axions can contribute to the hot dark matter component of the universe, together with the three active neutrinos. Axions have a free-streaming nature, suppressing structure formation at small scales, and also contribute to the dark radiation background, leading to deviations of the relativistic degrees of freedom N_{eff} from its canonically expected value of $N_{eff} = 3.046$.
- We constrained the thermal axion mass assuming that the underlying primordial perturbation power spectrum follows the usual power-law description, but also we have relaxed such an assumption, in order to test the robustness of the cosmological axion mass bounds, using an alternative, non-parametric description of the primordial power spectrum of the scalar perturbations, named PCHIP.
- The tightest bound we find in the PCHIP primordial power spectrum approach is obtained when considering BAO measurements together with CMB data, with $m_a < 0.89$ eV at 95% CL. In the standard power-law primordial power spectrum modeling, the same combination of data gives $m_a < 0.84$ eV at 95% CL.
- These bounds are very similar, confirming the robustness of the cosmological axion mass measurements versus the primordial power spectrum modeling.

We can conclude that the axion mass constraints are only mildly sensitive to the primordial power spectrum choice and therefore are not strongly dependent on the particular details of the underlying inflationary model.

References

- P. A. R. Ade et al. [Planck Collaboration], arXiv: 1303.5076 [astro-ph.CO];
- P. A. R. Ade et al. [Planck Collaboration], arXiv:1303.5080 [astro-ph.CO];
- P. A. R. Ade et al. [Planck Collaboration], arXiv:1502.01589 [astro-ph.CO];
- R. Adam et al. [Planck Collaboration], arXiv:1502.01582 [astro-ph.CO];
- G. Mangano et al., Nucl. Phys. B 729, 221 (2005) [hep-ph/0506164];
- R. D. Peccei and H. R. Quinn, Phys. Rev. Lett. 38, 1440 (1977);
- E. Giusarma et al., Phys. Rev. D90 (2014), 043507;
- L. Visinelli and P. Gondolo, arXiv:1403.4594 [hep-ph];
- D.J. Gross, R.D. Pisarski, and L.G. Yaffe, Rev. Mod. Phys. 53, 43 (1981);
- L. Visinelli and P. Gondolo, Phys. Rev. D 80, 035024 (2009);
- E. Di Valentino et al., Phys. Rev. D90 (2014), 023543.
- E. Di Valentino, S. Gariazzo, E. Giusarma, O. Mena,"Robustness of cosmological axion mass limits", Phys. Rev. D. 91, 123505 (2015), arXiv: 1503.00911.